doi.org/10.36721/PJPS.2026.39.11.325.1

Platycodon grandiflorus decoction against lipopolysaccharide (LPS)-induced acute lung injury via Keap1/Nrf2/ARE signaling pathway

Jia-Yi Zhang[1], Shu-Ting Zhang[1], Yang Yu[1,2,3], Ju-Tao Wang[1,2*] and Bai-Xiang Cai[1,2*]
[1]School of Pharmacy, Anhui University of Chinese Medicine, Hefei, PR China
[2]Anhui Province Key Laboratory of Bioactive Natural Products, Hefei, PR China
[3]Functional Activity and Resource Utilization on Edible and Medicinal Fungi Joint Laboratory of Anhui Province, Hefei, PR China

Abstract: **Background**: Acute lung injury (ALI)/acute respiratory distress syndrome (ARDS) is a severe inflammatory disease with high incidence and mortality rates. The traditional Chinese medicine *Platycodon grandiflorus* decoction (PGD) exerts protective effects against lipopolysaccharide (LPS)-induced ALI via the PI3K/AKT/NF-κB pathway, but its underlying molecular mechanisms require further elucidation. **Objectives**: This study aimed to investigate the molecular mechanism underlying the protective effects of PGD against LPS-induced ALI. **Methods**: *In-vivo* experiments employed an LPS-induced ALI mouse model to assess PGD's therapeutic potential. Complementary *in-vitro* studies examined the molecular mechanisms of PGD-enriched serum using human pulmonary epithelial (A549) and microvascular endothelial (HPMEC) cell lines. Nrf2 involvement in PGD-mediated protection was verified through siRNA-mediated gene silencing and subsequent functional validation. **Results**: Both *in-vitro* and *in vivo* analyses demonstrated that PGD effectively protects pulmonary tissues from LPS-induced damage. PGD administration notably enhanced Nrf2 nuclear translocation and decreased Keap1 expression at the protein and transcriptional levels, while promoting the expression of HO-1 and NQO1 biomarkers. Notably, Nrf2 gene silencing abolished PGD's therapeutic effects, including its anti-apoptotic properties. **Conclusions**: PGD's therapeutic efficacy in LPS-induced ALI is mediated through modulation of the Keap1/Nrf2/ARE signaling pathway.

Keywords: Acute lung injury; A549; HPMEC; Nrf2; Oxidative stress; *Platycodon grandiflorus* decoction

Submitted on 17-07-2025 – Revised on 12-08-2025 – Accepted on 09-12-2025

INTRODUCTION

ALI/ARDS remains a life-threatening condition with high incidence and fatality rates, drawing global attention to the urgent need for improved therapeutic strategies to enhance clinical outcomes (Dhar *et al*., 2021). With the evolution of therapeutic approaches for ALI/ARDS management, contemporary scientific research has shifted focus from traditional pharmaceutical development to the exploration of preventive pharmacological agents and dietary supplements (Li and Pauluhn, 2017; Cong, 2024).

PGD is a well-established traditional Chinese medicine known for its detoxification and lung-moisturizing properties (Liu *et al*., 2024). First documented in the medical classic "*Shang-han-lun*," PGD has long been used to treat lung diseases (Wu *et al*., 2023). The formula consists of two herbs: *P. grandiflorus* (Jacq.) A. DC. (Campanulaceae) and *Glycyrrhiza uralensis* Fisch. (Leguminosae), combined in a 1:2 ratio for disease treatment (Xu *et al*., 2022). Both plants are also used in daily tea preparations.

ALI is a severe respiratory condition characterized by uncontrolled lung inflammation (cytokine storm) due to massive leukocyte infiltration (Li *et al*., 2023; Jiang *et al*., 2023). This intense inflammatory response, driven by activated immune cells, generates excess reactive oxygen species (ROS) that overwhelm cellular antioxidant defenses. The resulting oxidative stress damages the pulmonary capillary endothelium and alveolar epithelium (Shi *et al*., 2023). The disruption of the blood-gas barrier, consisting of pulmonary microvascular endothelial cells and alveolar epithelial cells, is a hallmark of ALI (Ackermann *et al*., 2024). Respiratory epithelial cells play a pivotal role in innate immunity, serving as the primary defense against airborne pathogens (Traber and Mizgerd, 2025). Similarly, vascular endothelial cells contribute significantly to pathological processes, including inflammation, oxidative damage, structural vascular changes and coagulation abnormalities (Kunzmann *et al*., 2022). LPS, a component of Gram-negative bacterial membranes, is commonly used in experimental models to mimic ALI pathophysiology (Chen *et al*., 2022). During pulmonary damage progression, circulating neutrophils are recruited to the affected tissue, adhering to the vascular endothelial surfaces. These activated neutrophils release ROS and cytoplasmic components, further elevating oxidative stress markers and impairing endothelial function (Alekhmimi *et al*., 2023). The Keap1/Nrf2/ARE signaling axis serves as a critical cellular defense mechanism against oxidative stress. Nrf2 is a key transcriptional regulator of cytoprotective processes (Lee and Hu, 2020), acting as a central mediator in maintaining cellular homeostasis during oxidative stress (Ge *et al*., 2024). Under basal conditions, Nrf2 is sequestered in the cytoplasm, bound to its anchor protein, Keap1, through a constitutive interaction. Upon exposure to oxidative stress, kinase-

**Corresponding author:* e-mail: wjt591@ahtcm.edu.cn ; caibx@ahtcm.edu.cn

mediated phosphorylation triggers the release of Nrf2 from this complex, allowing its translocation to the nucleus. Once in the nucleus, activated Nrf2 binds to ARE sequences to drive the transcription of phase II detoxification enzymes and antioxidant proteins, including heme oxygenase-1 (HO-1) and NAD(P)H quinone oxidoreductase 1 (NQO1), as demonstrated in recent mechanistic studies (Huang *et al*., 2023).

Recent research into the Keap1/Nrf2/ARE signaling axis has highlighted the protective and therapeutic effects of various compounds against ALI. Experimental data show that ellagic acid mitigates oxidative damage in neuronal models of Parkinson's disease by inhibiting Keap1, thereby promoting Nrf2 nuclear accumulation and activating the synthesis of ARE-driven proteins (Wang *et al*., 2022). Curcumin, known for its broad pharmacological effects, including anti-inflammatory, antioxidant and immunomodulatory properties (Jiang *et al*., 2017), significantly reduces doxorubicin-induced neurotoxicity by modulating autophagy, oxidative stress and endoplasmic reticulum homeostasis (Li *et al*., 2019). Andrographolide, a major bioactive compound from Andrographis paniculata, protects against oxidative stress in chondrocytes. In H_2O_2-induced damage models, this diterpenoid activates the Keap1-Nrf2-ARE pathway, promoting cellular proliferation and restoring antioxidant enzyme activity impaired by oxidative stress (Liao *et al*., 2023). Preliminary phytochemical analysis using ultra-high-performance liquid chromatography coupled with quadrupole time-of-flight tandem mass spectrometry (UPLC-Q-TOF-MS/MS) identified 70 distinct constituents in the study material. These included 33 flavonoid derivatives, such as glycyrrhizin, coriander in and bilobalamin, 8 terpenoid compounds, including glycyrrhetinic acid, 3 saponin derivatives (platycodonin E and D), 6 phenolic acid derivatives, 5 amino acids, 5 glycosides, 3 phenylpropanoids, 2 alkaloids and 5 miscellaneous components. Together, these constituents may form the pharmacodynamic foundation of PGD (Xuan *et al*., 2024).

Previous studies by our research team have demonstrated the anti-inflammatory effects of PGD in experimental models. PGD was shown to reduce pro-inflammatory cytokines, such as tumor necrosis factor-α (TNF-α), interleukin-1β (IL-1β) and interleukin-6 (IL-6), in murine models of ALI. Additionally, PGD effectively alleviated LPS-induced ALI (Xuan *et al*., 2024). Building on these findings, the present study investigates the therapeutic potential of PGD against LPS-induced pulmonary damage and elucidates its molecular mechanisms through modulation of the Keap1/Nrf2/ARE signaling cascade.

MATERIALS AND METHODS

Reagents and antibodies

LPS and dexamethasone (DEX) were obtained from Sigma-Aldrich (St. Louis, MO, USA). *P. grandiflorus* (Jacq.) A. DC. and *G. uralensis* Fisch. were sourced from Anhui Minshuntang Chinese Medicine Technology Co. (Xianju, China). Primary antibodies against Keap1, Nrf2, HO-1 and NQO1, as well as secondary antibodies (HRP-conjugated goat anti-rabbit IgG(H+L) and goat anti-mouse IgG(H+L)), were purchased from Affinity Biosciences (OH, USA). β-actin antibodies were sourced from Beijing Zhongshan Golden Bridge Biotechnology Co., Ltd. (Beijing, China).

Preparation of PGD

P. grandiflorus (Jacq.) A. DC. and *G. uralensis* Fisch. (1:2) were immersed in a 12-fold volume of aqueous solvent for initial extraction. The herbal mixture was subjected to sustained thermal treatment until boiling, followed by a secondary extraction of the marc using 10 volumes of purified water. Both aqueous extracts were pooled, filtered, vacuum-concentrated and diluted to prepare graded concentrations of JGD solutions (1.95 g/mL, 0.975 g/mL and 0.4875 g/mL), corresponding to 39 g/kg, 19.5 g/kg and 9.75 g/kg body weight of raw herb, respectively (Xuan *et al*., 2024).

Animals

Male C57BL/6 mice (aged 8–10 weeks, body weight 20 ± 2 g) were purchased from Ziyuan Experimental Animal Technology Co., Ltd. (Hangzhou, China). The mice were group-housed (n = 8/cage) in controlled conditions (ambient temperature 23 ± 2°C, relative humidity 50 ± 10%) under a standardized 12-hour light/dark cycle and maintained in specific pathogen-free conditions.

ALI murine model

The ALI murine model was established using standardized protocols (Xuan *et al*., 2024). The animals were divided into six randomized groups based on body weight: control, LPS, LPS + DEX (1.17 mg/kg), LPS + PGD-H (39 g crude drug/kg), LPS + PGD-M (19.5 g crude drug/kg) and LPS + PGD-L (9.75 g crude drug/kg). Both control and LPS groups received distilled water *via* oral gavage (0.2 mL per 10 g body weight) daily for seven consecutive days. One hour after the final dose, animals were anesthetized and non-control groups underwent intratracheal LPS instillation (5 mg/kg), while control animals received equivalent volumes of PBS. Biological specimens (serum and lung tissues) were collected post-euthanasia after LPS exposure.

Wet/dry (W/D) ratios

Freshly excised pulmonary tissues were immediately subjected to gravimetric analysis of the left upper lobe's wet weight to minimize moisture loss. Subsequently, tissues were dried in a 60°C convection oven until a constant dry weight was achieved. The wet-to-dry weight ratio was calculated as a quantitative indicator of interstitial fluid accumulation in the lungs.

Histopathological examination

Lung specimens were fixed in 4% paraformaldehyde for at

least 48 hours, then subjected to sequential ethanol dehydration and paraffin embedding. Thin sections (4 μm) were prepared and stained using the hematoxylin-eosin (H and E) protocol. Microscopic analysis was performed to assess morphological changes in pulmonary architecture.

Preparation of PGD-containing serum

A cohort of forty male C57BL/6 mice was randomly allocated into two experimental groups: a control serum group (n = 10) and a PGD-supplemented serum group (n = 30). The PGD-treated group received daily oral administration of PGD suspension (39 g/kg body weight) for seven consecutive days, while control mice were administered equivalent volumes of aqueous solvent. Six hours after the final treatment, blood samples were collected and processed using sequential protocols: initial refrigeration at 4°C for 2 hours, followed by centrifugation (3000 rpm, 20 minutes) to isolate cell-free serum. Supernatants from each group were pooled, sterile-filtered through 0.22 μm membranes, heat-inactivated at 56°C for 30 minutes and then cryopreserved at -20°C after aliquot preparation.

Cell culture

Human non-small cell lung cancer cells (A549, Bluefcell, Shanghai, China) were cultured in Ham's F-12K medium (Procell, Wuhan, China) supplemented with 10% heat-inactivated fetal bovine serum (Procell) and 1% penicillin-streptomycin solution (Wisent, Nanjing, China), with routine incubation at 37°C in a 5% CO_2 atmosphere. Human Pulmonary Microvascular Endothelial Cells (HPMEC, Procell) were cultured in Dulbecco's modified Eagle's medium (DMEM, Wisent, Nanjing, China), supplemented with 10% heat-inactivated FBS and 1% penicillin-streptomycin, under identical culture conditions.

Before experimental treatments, all cell lines were preconditioned for 24 hours with varying concentrations of PGD-supplemented serum, followed by a 12-hour LPS stimulation as per experimental design requirements.

Cell viability assay

Cell viability was assessed using the Cell Counting Kit-8 (CCK-8, Biosharp, Hefei, China). HPMEC cells were seeded into 96-well plates at a density of 1×10^4 cells/well and exposed to different concentrations (0%, 2%, 5%, 10%, 15%, 20%) of PGD-supplemented or control serum for 24 hours. Concurrently, A549 cells were cultured in 96-well plates at 5×10^4 cells/well and treated with equivalent serum concentrations (0%, 2%, 5%, 10%, 15%, 20%). After 24 hours, 10 μL of CCK-8 solution was added to each well, followed by incubation at 37°C for 90 minutes. Optical density was measured at 450 nm to assess cell viability.

Additionally, cells were exposed to varying concentrations of LPS (0, 0.1, 0.5, 1, 5 μg/mL) for treatment periods of 6, 12 and 24 hours. After treatment, 10 μL of CCK-8 reagent was added to each well, followed by incubation under standard conditions. Optical density at 450 nm was recorded to calculate cellular viability, allowing determination of the optimal LPS treatment parameters through data analysis.

Determination of MDA, SOD and GSH-PX levels

Malondialdehyde (MDA) concentration, along with the enzymatic activities of superoxide dismutase (SOD) and glutathione peroxidase (GSH-PX), were quantified using commercial assay kits (Nanjing Jiancheng Bioengineering Institute, Jiangsu, China) according to standardized protocols for both *in-vitro* and *in-vivo* studies.

Detection of ROS

A549 and HPMEC cell lines were cultured in 24-well plates for 24 hours. After treatment, cells were harvested, rinsed three times with PBS and incubated with 10 μM dichlorodihydrofluorescein diacetate (DCFH-DA, Jiancheng, Nanjing, China) under light-protected conditions for 20 minutes. After three additional PBS washes to remove excess probe, cellular fluorescence signals were captured using a microscopic imaging system.

Immunofluorescence staining

Following a 24-hour incubation, A549 and HPMEC cell lines were plated in 24-well culture plates. The cells were fixed using 4% paraformaldehyde solution at 37°C for 20 minutes. Membrane permeabilization was performed with 0.5% Triton X-100 for 30 minutes, followed by three PBS washes. Blocking was achieved with 2% bovine serum albumin for 60 minutes at 37°C. Primary antibodies were incubated overnight at 4°C, followed by PBS rinsing and a 2-hour exposure to fluorescent secondary antibodies at 37°C. Nuclear visualization was performed using 4',6-diamidino-2-phenylindole (DAPI, Beyotime, Shanghai, China) staining and the slides were mounted with anti-fade mounting medium for fluorescence microscopy.

siRNA transfection

A549 and HPMEC cells were transfected with siRNA using the ribo*FECT*™ CP Transfection Kit (Ribobio, Guangzhou, China) according to the supplier's instructions. Cells were transfected with either Nrf2-targeting siRNA or scrambled control siRNA for 48 hours. After transfection, the medium was replaced with standard culture medium. Cellular RNA from each treatment group (Table S1) was isolated and Nrf2 mRNA levels were measured using RT-qPCR to determine the most effective siRNA sequence.

Real-time quantitative PCR (RT-qPCR) analysis

Total RNA was extracted from pulmonary tissue and cell samples using Trizol reagent, followed by cDNA synthesis using the Biosharp kit according to the manufacturer's instructions. The RT-qPCR protocol involved an initial 95°C denaturation for 2 minutes, followed by 40 cycles of

denaturation at 95°C for 15 seconds and annealing/extension at 60°C for 30 seconds, with a melting curve analysis from 60°C to 95°C. Quantitative data were represented as cycle threshold (C.T.) values normalized to *β*-actin, with differential expression calculated using the $2^{-\Delta\Delta}$Ct method. Specific primer sequences are listed in table S2.

Western blot analysis

Total protein was isolated from pulmonary tissue and cell lysates using RIPA lysis buffer. Protein concentrations were measured using a BCA assay kit (Beyotime) before loading equal amounts onto SDS-PAGE gels for electrophoretic separation. Separated proteins were transferred onto PVDF membranes and blocked for 2 hours. Membranes were incubated overnight at 4°C with primary antibodies targeting Keap1, Nrf2, HO-1, NQO1 and β-actin. After primary antibody incubation, membranes were probed with HRP-conjugated secondary antibodies (Goat anti-rabbit or anti-mouse IgG(H+L)) and developed using ECL chemiluminescent substrate (Beyotime). Quantitative analysis was performed by normalizing the target protein expression to β-actin levels and measuring the grayscale intensities using ImageJ software.

Apoptosis assay

Cell apoptosis was evaluated using the Annexin V-FITC Detection Kit (Beyotime, Shanghai, China) according to standard protocols. After two washes with cold PBS, cell suspensions were prepared at a concentration of 1×10^6 cells/mL. The samples were stained with 5μL FITC annexin V and 5 μL propidium iodide (PI) and incubated in the dark at 4°C for 15 minutes. Flow cytometric analysis was performed on a BD LSRFortessa system (Franklin Lakes, NJ, USA), with data analysis conducted using Flowjo10 software.

Statistical analysis

Quantitative data are presented as mean ± standard deviation. Group comparisons were performed using GraphPad Prism 9.5 (CA, USA) software, applying appropriate statistical tests such as one-way ANOVA and two-tailed Student's t-test. A *P*-value of < 0.05 was considered statistically significant.

RESULTS

PGD attenuates inflammation and oxidative stress and regulates Keap1/Nrf2/ARE pathway in LPS-induced ALI mice

The effects of PGD administration on LPS-induced pulmonary injury were systematically evaluated. The results are summarized in fig. 1. Histopathological analysis using H&E staining revealed significant pulmonary damage following LPS exposure. Compared to control specimens, this damage was characterized by interstitial edema, a marked accumulation of neutrophils and pronounced thickening of the alveolar septa. Therapeutic interventions with varying doses of PGD (9.75 mg, 19.5 mg, or 39 mg of crude drug/kg) and DEX alleviated pulmonary damage in a dose-dependent manner. This was evidenced by reduced tissue edema, decreased leukocyte infiltration and restored alveolar septal structure (Fig. 1a) Quantitative analysis showed a significant increase in the pulmonary wet-to-dry weight ratio after LPS challenge (Fig. 1b). Both histopathological scoring and hydrostatic measurements confirmed a significant reduction in pulmonary injury compared to the LPS-treated group. PGD pretreatment effectively decreased lipid peroxidation (MDA levels), increased GSH-PX levels and restored SOD activity in both pulmonary tissue and systemic circulation (Figs. 1c-1h). These results suggest that PGD pretreatment provides protective effects against LPS-induced ALI by enhancing antioxidant defenses and modulating inflammatory responses.

Comparative analysis revealed a significant upregulation of Nrf2, HO-1 and NQO1 transcriptional activity in both the PGD-H (39 g/kg) and DEX groups ($P < 0.05$). The expression of these markers increased progressively with the PGD concentration (Figs. 1i-1l). Experimental data indicated that PGD intervention effectively inhibited Keap1 protein synthesis, while also upregulating Nrf2, NQO1 and HO-1 expression compared to the LPS-challenged group. These results provide mechanistic evidence for PGD's activation of the Keap1/Nrf2/ARE regulatory network (Fig. 1m, Figs. S1a-S1d).

PGD-containing serum pretreatment modulated the Keap1/Nrf2/ARE signaling pathway and protected against LPS-induced injury

Experimental data from CCK-8 assays revealed that serum containing PGD at various concentrations (0%, 2%, 5%, 10%, 15%, 20%) did not exhibit significant cytotoxicity (Figs. S2a and S2b). Notably, cellular viability was significantly reduced in both HPMEC and A549 cell lines when exposed to 20% PGD-containing serum. Based on these results, three experimental groups were established for further investigations: 15% PGD as the high-concentration treatment, with 10% and 5% serving as intermediate and low concentrations, respectively. The CCK-8 analysis also identified the optimal experimental parameters: a 12-hour exposure duration at 1 μg/mL, which was adopted for all subsequent studies (Figs. S2c and S2d).

ROS are critical mediators of cellular damage mechanisms in ALI. Under normal physiological conditions, ROS are involved in essential cellular signaling and defense processes. However, excessive ROS production can lead to macromolecular degradation, including oxidative modifications of proteins, lipid peroxidation and DNA strand breaks (Escobar *et al*., 2024). Oxidative stress has been confirmed as a central factor in the pathogenesis of ALI (Wang *et al*., 2024).

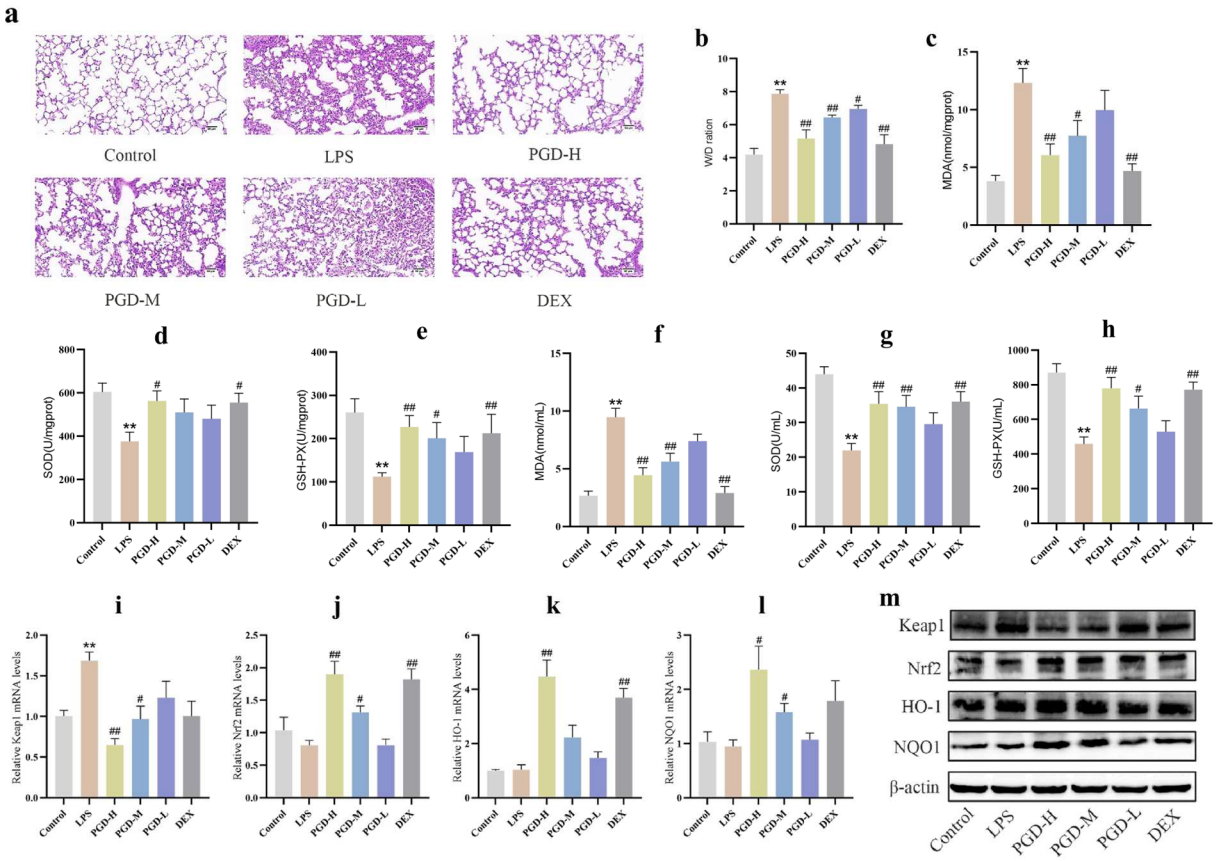

Fig. 1: PGD attenuates inflammation and oxidative stress and upregulates Keap1/Nrf2/ARE pathway in LPS-induced ALI mice. The representative images for the histopathological changes (H & E staining) in the (a) lung tissues, (b) lung W/D ratio, (c) MDA, (d) the SOD and (e) GSH-PX activity in lung tissues, (f) the MDA, (g) SOD and (h) GSH-PX activity in serum, mRNA levels of Keap1(i), Nrf2(j), HO-1(k) and NQO1(l) mRNA in lung tissue and protein expression of Keap1, Nrf2, HO-1 and NQO1 in lung tissue(m). All data are expressed as mean ± S.D. $^{**}p < 0.01$ vs. control group, $\#p < 0.05$; $\#\#p < 0.01$ vs. LPS alone group.

In the present study, the therapeutic serum with 15% PGD significantly enhanced antioxidant defenses, evidenced by decreased MDA levels, increased GSH-PX concentrations and restored SOD enzymatic activity (Figs. 2a-2f). LPS-activated cells showed a significant increase in ROS levels, which was effectively mitigated by PGD treatment, as demonstrated by immunofluorescence analysis (Figs. 2g-2i). Quantitative analysis also showed significant nuclear translocation of the Nrf2 transcription factor in PGD-treated groups ($P < 0.01$). Enhanced fluorescence intensity and density indicated increased activation of the antioxidant response element (ARE) (Figs. 2j-2l).

Additionally, compared to control conditions, significantly elevated Keap1 protein levels were observed in LPS-treated samples. PGD-containing serum formulations exerted concentration-dependent regulatory effects on the Keap1/Nrf2/ARE pathway. Specifically, the 15% PGD serum group effectively suppressed Keap1 expression while enhancing the expression of Nrf2, HO-1 and NQO1, compared to LPS-challenged cells. This modulation of the pathway underpins the protective effect of PGD against LPS-induced cellular damage in both HPMEC and A549 models (Figs. 2m and 2n, Figs. S3a-S3h).

siNrf2 reversed the anti-lung injury and oxidative stress effects of PGD in A549 and HPMEC cells

To investigate the regulatory mechanisms of the Keap1/Nrf2/ARE pathway in mitigating pulmonary damage and oxidative stress through PGD, Nrf2 gene silencing was performed *via* transfection. The results showed that, compared to cells treated with 15% PGD-containing serum, the siNrf2-pretreated group exhibited significantly increased ROS and MDA levels, along with significantly decreased SOD and GSH-PX activities (Figs. 3a-3f).

Immunofluorescence imaging revealed a marked reduction in fluorescence intensity and a decrease in Nrf2 nuclear translocation in the gene-silenced group compared to the PGD-treated groups (Figs. 3g-3m). These findings highlight the essential role of Nrf2 in mediating the therapeutic effects of PGD against pulmonary injury and oxidative stress.

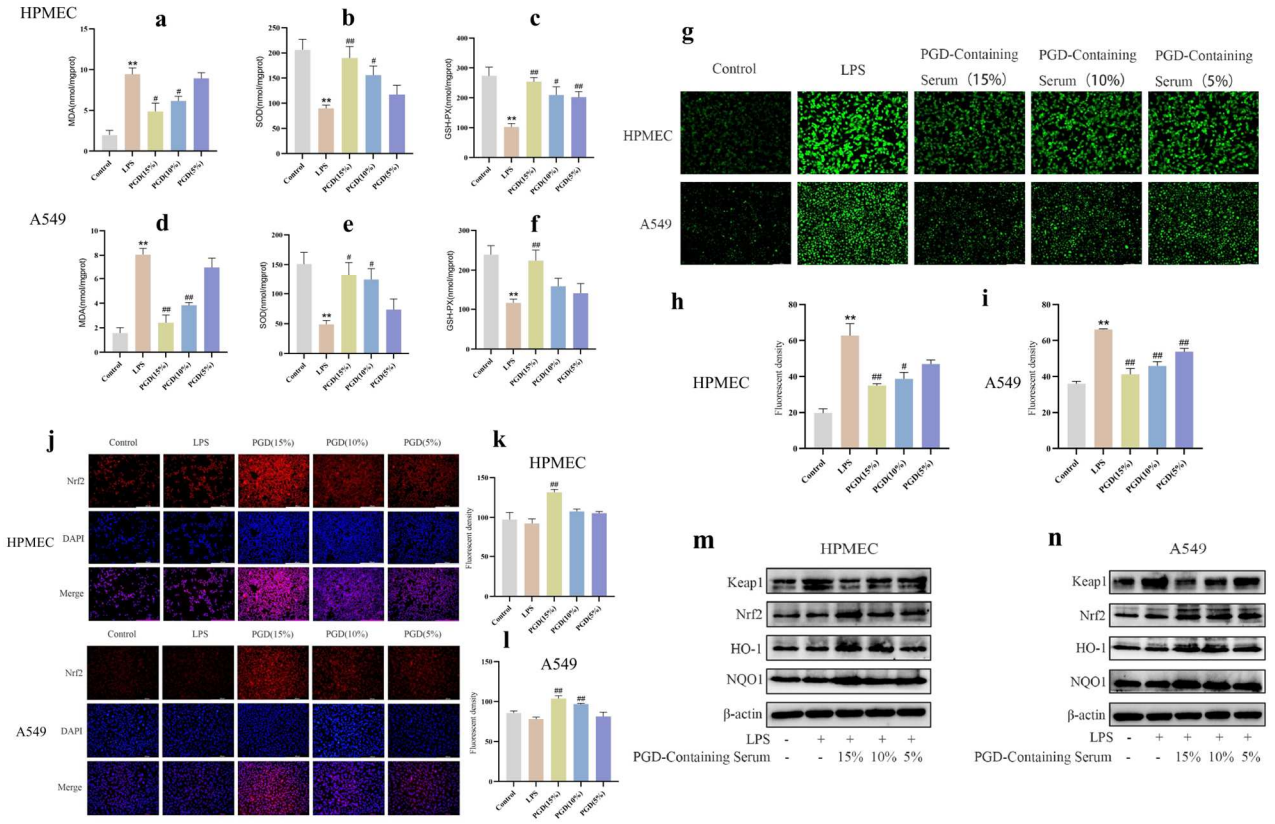

Fig. 2: PGD-containing serum pretreatment modulated the Keap1/Nrf2/ARE signaling pathway and protected against LPS-induced ALI. Detection of (a) MDA, (b) SOD and (c) GSH-PX in HPMEC cell, detection of (d) MDA, (e) SOD and (f) GSH-PX in A549 cells, (g) representative ROS staining in HPMEC and A549 cells, ROS fluorescence density in (h) HPMEC and (i) A549 cells, (j) nuclear protein expression of Nrf2, fluorescence density analysis of Nrf2 into nuclei in (k) HPMEC and (l) A549 cells and protein expression of Keap1, Nrf2, HO-1 and NQO1 protein in (m) HPMEC and (n) A549 cells. The data are expressed as mean ± S.D. $^{**}p < 0.01$ vs. control group; $\#p < 0.05$, $\#\#p < 0.01$ vs. LPS alone group.

RT-qPCR experiments revealed that siNrf2 reversed the therapeutic effects of PGD on pulmonary injury and oxidative stress in both HPMEC and A549 cells. Screening for silencing efficiency identified siRNA-2 (target sequence: GCTACGTGATGAAGATGGA) as the most effective in silencing Nrf2 expression compared to other siRNA variants (Figs. S4a-S4b).

Nrf2 plays a key role in PGD exerting anti-lung injury and oxidative stress effects

RT-qPCR and immunoblotting analyses indicated that, compared to the PGD (15%)-enriched serum group, Keap1 expression at both the transcriptional and translational levels was significantly increased, while Nrf2, HO-1 and NQO1 were markedly downregulated (Figs. 4a-4j, Figs. S5a-S5h). The serum containing 15% PGD significantly reduced LPS-induced apoptosis. Comparative analysis showed enhanced apoptotic activity in the PGD (15%) + siNrf2 group compared to the PGD (15%) group (Figs. 4k-4m). Genetic inhibition of Nrf2 using siRNA effectively negated the protective effects of PGD-enriched serum against LPS-induced pulmonary damage. Collectively, these results suggest that PGD-infused serum exerts therapeutic effects against pulmonary injury and oxidative stress by activating the Nrf2 pathway, thereby safeguarding the cellular integrity of HPMEC and A549 cells from LPS-induced cytotoxicity.

DISCUSSION

During pulmonary inflammation, respiratory epithelial and vascular endothelial cells collaborate to maintain tissue homeostasis and immune balance within the lungs (Silwedel *et al*., 2019). The alveolar structure consists of specialized epithelial cells that form an initial barrier between external environmental factors and internal physiological spaces. Experimental evidence has shown that disruption of this protective interface is a critical factor in various pulmonary diseases, such as acute respiratory distress syndrome and lung trauma (Willems *et al*., 2013; Zhao *et al*., 2025). Serving as the primary defense mechanism against environmental insults, the alveolar epithelium is vital for preserving the integrity of the air-blood barrier (Liu *et al*., 2023).

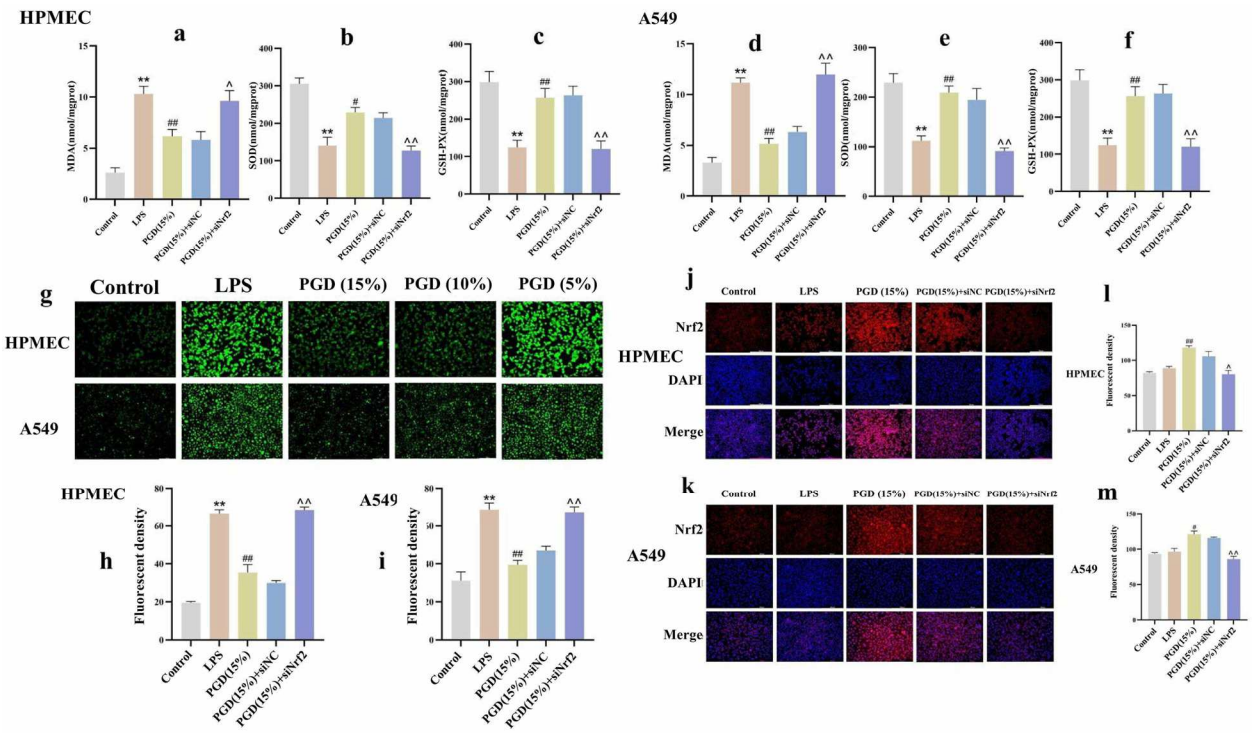

Fig. 3: siNrf2 reversed the anti-lung injury and oxidative stress effects of PGD in A549 and HPMEC cells. (a-f) Detection of MDA, SOD, GSH-PX in siNrf2 HPMEC and A549 cells; (g) representative ROS staining, ROS fluorescence density in siNrf2; (h) HPMEC and; (i) A549 cells; (j-k) nuclear protein expression of Nrf2, fluorescence density analysis of Nrf2 into nuclei in siNrf2; (l) HPMEC and; (m) A549 cells. The data are expressed as mean ± S.D. $**p < 0.01$ vs. control group; $\#p < 0.05$, $\#\#p < 0.01$ vs. LPS alone group; $\hat{}p < 0.05$, $\hat{}\hat{}p < 0.01$ vs. PGD (15%) group.

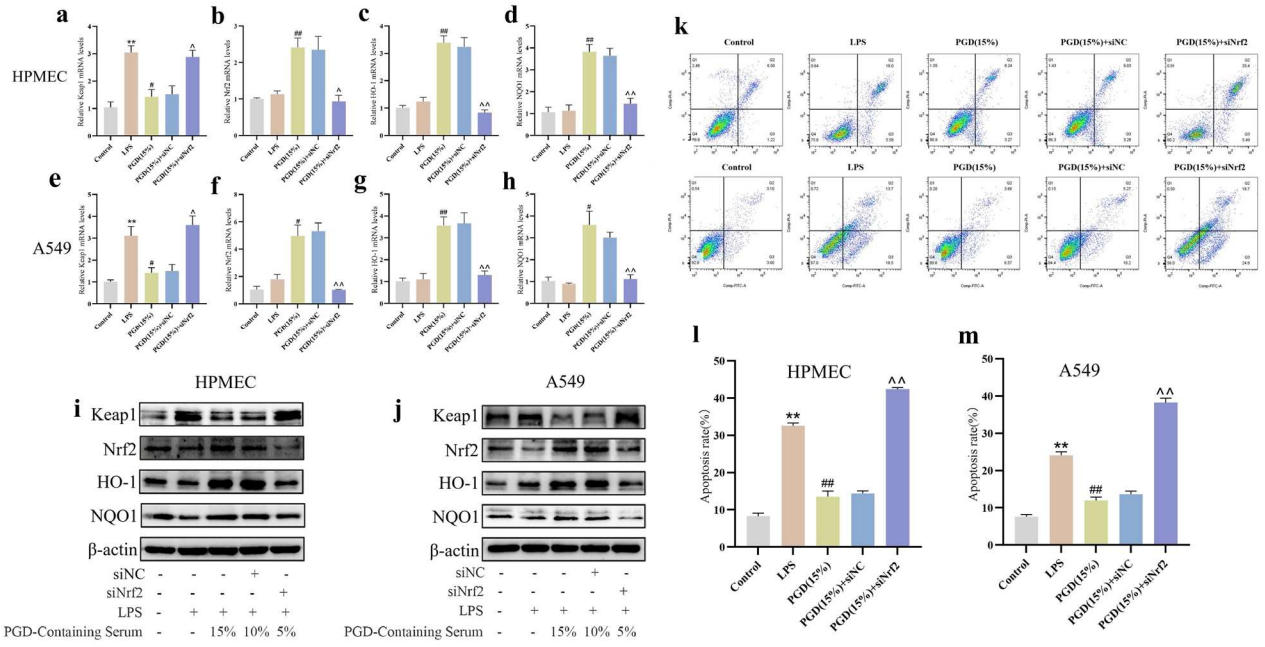

Fig. 4: Nrf2 plays a key role in PGD exerting anti-lung injury and oxidative stress effects. (a-d) mRNA levels of Keap1, Nrf2, HO-1, (e-h) NQO1 in siNrf2 HPMEC and A549 cells, protein expression of Keap1, Nrf2, HO-1, NQO1 in siNrf2 (i) HPMEC and (j) A549 cells, cell apoptosis and necrosis distribution in (k) HPMEC and A549 cells and apoptosis rates in (l) HPMEC and (m) A549 cells. The data are expressed as mean ± S.D. $**p < 0.01$ vs. control group; $\#p < 0.05$, $\#\#p < 0.01$ vs. LPS alone group; $\hat{}p < 0.05$, $\hat{}\hat{}p < 0.01$ vs. PGD (15%) group.

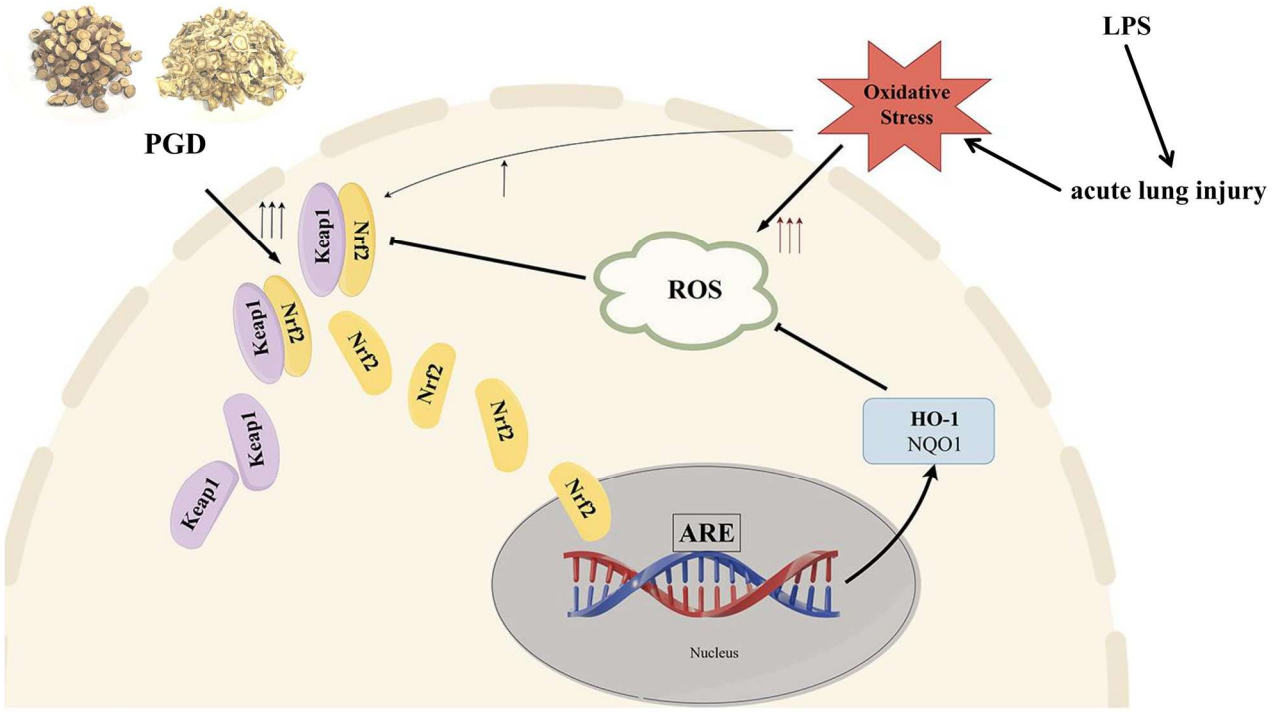

Fig. 5: Mechanism of action of PGD. The symbol"⊥" refers to down-regulation and the symbol "↑" refers to up-regulation. LPS induces the production of ALI, leading to oxidative stress. When oxidative stress is activated, it promotes ROS production while dissociating Nrf2 from Keap1 and transferring it to the nucleus. The incoming Nrf2 binds to the ARE to initiate transcription of antioxidant proteins such as HO-1 and NQO1.PGD inhibits ROS production by regulating the Keap1/Nrf2/ARE signaling pathway, thereby resisting injury and oxidative stress.

The preservation of pulmonary endothelial cells is essential for maintaining hemodynamic stability in both pulmonary and systemic vascular networks. Pathological alterations in lung microvascular endothelial cells, particularly apoptosis, are significant contributors to the development of ALI (Wu *et al*., 2020). Alveolar epithelial type II cells (AECII), which make up approximately 60% of the alveolar epithelial cells and 10-15% of all pulmonary cells, play pivotal roles in epithelial maintenance and regeneration. The extent of pulmonary damage is closely linked to structural and functional impairments in these cells. In particular, combined injury to both alveolar capillaries and epithelial layers accelerate the pathological progression of lung damage (Xu *et al*., 2020). The A549 cell line, widely used as an *in vitro* model, shares several key biological characteristics with native AECII cells (Meldrum *et al*., 2022). Recent studies highlight oxidative stress as a central mechanism in the pathogenesis of LPS-induced ALI (Al-Joufi *et al*., 2024), suggesting that targeting oxidative damage and inflammatory cascades may help mitigate pulmonary deterioration. Experimental results demonstrated that PGD administration effectively alleviated oxidative stress. The compound exerted protective effects by reducing the severity of pulmonary edema and improving histopathological damage in lung tissues. Biochemical analysis revealed that PGD significantly decreased MDA levels while enhancing the enzymatic activities of SOD and GSH-PX. These findings suggest that PGD's mechanism of action likely involves regulating the redox balance, inhibiting lipid peroxidation and enhancing endogenous antioxidant defenses in lung injury models.

The transcription factor Nrf2, encoded by the *NFE2L2* gene, is a member of the CNC family of leucine zipper transcription factors (Dinkova and Copple, 2023). As a key mediator of the oxidative stress response, Nrf2 regulates the balance of intracellular ROS, maintains redox homeostasis and protects cells from cytotoxicity induced by free radicals (Hsu *et al*., 2022). Nrf2 activates a range of antioxidant defense genes, including NQO1, HO-1, thioredoxin reductase 1 and SOD 1, through transcriptional regulation *via* the ARE (Li *et al*., 2022). Research has identified Kelch-like ECH-associated protein 1 (Keap1) as a key negative regulator of the Nrf2 pathway, forming the Keap1-Nrf2-ARE axis (Ulasov *et al*., 2022). Under basal conditions, Keap1 facilitates the cytoplasmic retention and proteasomal degradation of Nrf2 through ubiquitination (Meldrum *et al*., 2022). Nrf2 plays a pivotal role in regulating cellular redox balance, iron homeostasis, xenobiotic biotransformation and protein quality control (Guan *et al*., 2024; Islam *et al*., 2023). Experimental data show that Nrf2 is highly expressed in the lungs and regulates inflammatory responses in pneumonia models.

Impaired Nrf2 signaling exacerbates lung tissue damage during inflammation, while pharmacological activation provides organ-protective effects (Murakami *et al*., 2023; Chen *et al*., 2020). These findings suggest that Nrf2 could serve as a potential therapeutic target for respiratory diseases (Shakya *et al*., 2024).

This study utilized both *in-vivo* and *in-vitro* approaches to investigate the protective mechanisms of PGD against pulmonary damage. In animal models, pretreatment with orange broth was applied before inducing LPS-induced lung injury. In cellular studies, PGD-enriched serum pretreatment was conducted before exposing HPMEC and A549 cells to LPS. Both experimental models demonstrated consistent protective outcomes. Immunofluorescence analysis revealed enhanced nuclear translocation of Nrf2 following PGD serum administration. These results suggest that PGD alleviates oxidative stress by modulating the Keap1/Nrf2/ARE pathway, providing protection against LPS-induced ALI. Initial mechanistic studies imply that PGD regulates this antioxidant pathway by upregulating Nrf2 expression and downregulating Keap1 levels, thereby activating downstream protective genes such as HO-1 and NQO1. As shown in fig. 5, PGD exerts protective effects on cellular and tissue structures by mitigating oxidative stress-induced damage during pulmonary injury events.

The Nrf2 signaling axis presents a paradoxical duality: while it protects healthy cells from oxidative stress, it also shields malignant cells from therapeutic interventions (Gong *et al*., 2024). This pathway contributes to cancer progression by promoting cellular proliferation, metastasis and resistance to treatments. Cancers driven by this pathway are classified as Nrf2-dependent malignancies (Hayashi *et al*., 2020). Currently, pharmacological strategies targeting this pathway remain experimental. In chemoprevention research, efforts focus on identifying Nrf2 activators and inhibitors of its downstream targets to address oxidative stress-related diseases. Emerging evidence suggests that precise modulation of Nrf2 transcriptional activity may reduce its oncogenic potential (Liu *et al*., 2021). siRNA-mediated gene silencing demonstrated that Nrf2 knockdown abolished the protective effects of PGD-containing serum against ALI, confirming its regulatory role in the Keap1/Nrf2/ARE pathway in alleviating ALI.

The Keap1/Nrf2/ARE pathway is vital in mitigating inflammatory responses and oxidative stress-induced damage, while eliminating excess ROS, thereby offering therapeutic potential against ALI/ARDS (Tu *et al*., 2019). Our results further demonstrate that PGD administration protects against LPS-induced ALI through modulation of this signaling cascade.

While previous studies have characterized the phytochemical profile of PGD, the bioactive compounds in PGD-containing serum remain unidentified. These pharmacologically active components require further investigation and validation through subsequent analytical studies.

CONCLUSION

This study examined the effects of PGD on LPS-induced oxidative stress using both *in-vivo* and *in-vitro* approaches. The results indicate that PGD administration before LPS exposure significantly alleviates cellular damage and oxidative stress, showing considerable therapeutic potential for ALI. Mechanistic investigations suggest that the protective effects of PGD involve the modulation of the Keap1/Nrf2/ARE signaling axis. Our preliminary research establishes a crucial foundation for future pharmaceutical development and clinical applications. These findings not only confirm PGD's effectiveness in combating LPS-induced ALI but also suggest that its beneficial effects are linked to the precise regulation of redox-sensitive signaling pathways, providing a molecular basis for developing novel treatment strategies for ALI.

Acknowledgments
None.

Authors' contributions
Ju-Tao Wang and Bai-Xiang Cai: Study concepts; Jia-Yi Zhang, Ju-Tao Wang and Bai-Xiang Cai: Study design; Shu-Ting Zhang and Yang Yu: Literature research; Jia-Yi Zhang and Shu-Ting Zhang: Experimental studies; Jia-Yi Zhang and Shu-Ting Zhang: Data acquisition; Shu-Ting Zhang and Yang Yu: Data analysis; Shu-Ting Zhang and Yang Yu: Statistical analysis; Jia-Yi Zhang: Manuscript preparation; Jia-Yi Zhang, Ju-Tao Wang and Bai-Xiang Cai: Manuscript editing; Ju-Tao Wang and Bai-Xiang Cai: Manuscript review.

Funding
This work was supported by the Natural Science Research Program of Department of Education Anhui Province (2025AHGXZK40340), Excellent Youth Scientific Research Project of Anhui Province University (2024AH030031), The Open Fund of High-level Key Discipline of Chemistry of Chinese Medicine of the State Administration of Traditional Chinese Medicine, Anhui University of Chinese Medicine (HKDCCM2024012), Talent Support Program of Anhui University of Chinese medicine (2023rczd008).

Data availability statement
Data and materials will be made available on request.

Ethical approval
Animal studies were approved by the Animal Ethics Committee of Anhui University of Chinese Medicine (Permit number: AHUCM-mouse-2022038). This study

was performed in adherence with the ARRIVE guidelines. See supplementary file for the ARRIVE checklist.

Conflict of interest

The authors declare no conflict of interest.

Supporting information

Supplementary data associated with this article can be found in the attachment.

Supplementary data

https://pjps.pk/uploads/2026/08/SUP1787208641.pdf

REFERENCES

Ackermann M, Werlein C, Plucinski E, Leypold S, Kuehnel MP, Verleden SE, Khalil HA, Laenger F, Welte T, Mentzer SJ and Jonigk DD (2024). The role of vasculature and angiogenesis in respiratory diseases. *Angiogenes*, **27**(3): 293–310.

Alekhmimi NK, Cialla-May D, Ramadan Q, Eissa S, Popp J, Al-Kattan K and Zourob M (2023). Biosensing platform for the detection of biomarkers for ALI/ARDS in bronchoalveolar lavage fluid of lps mice model. *Biosensors-Basel.*, **13**(7): 676.

Al-Joufi, FA, Shaukat S, Hussain L, Khan K.ur R, Hussain N, Al Haddad AHI, Alqahtani A, Alqahtani T, Momenah MA, Ibrahim SA and Hussain M (2024). Lavandula stoechas significantly alleviates cigarette smoke-induced acute lung injury via modulation of oxidative stress and the NF-κB pathway. *Food Biosci.*, **59**: 103834.

Chen J, Huang Y, Bian X and He Y (2022). Berberine ameliorates inflammation in acute lung injury via NF-κB/Nlrp3 signaling pathway. *Front Nutr.*, **9**: 851255.

Chen Y, Evankovich J W, Lear TB, Tuncer F, Kennerdell JR, Camarco DP, Shishido MS, Liu Y and Chen BB (2020). A small molecule NRF2 activator BC-1901S ameliorates inflammation through DCAF1/NRF2 axis. *Redox Biol*., **32**: 101485.

Cong B (2024). Perspectives in food and medicine homology. *Food & Med Homology*, **1**: 9420018.

Dhar R, Rana MN, Zhang L, Li Y, Li N, Hu Z, Yan C, Wang X, Zheng X, Liu H, Cui H, Li Z and Tang H (2021). Phosphodiesterase 4B is required for NLRP3 inflammasome activation by positive feedback with Nrf2 in the early phase of LPS- induced acute lung injury. *Free Radic Biol Med*., **176**: 378–391.

Dinkova-Kostova AT and Copple IM (2023). Advances and challenges in therapeutic targeting of NRF2. *Trends Pharmacol Sci*., **44**(3): 137-149.

Escobar M, Fajardo C, Riano R, Barrios O, Zabala B, Muñoz R, Rivera E (2024). miRNAs involvement in modulating signalling pathways involved in ros-mediated oxidative stress in melanoma. *Antioxidants (Basel)*. **13**(11): 1326.

Ge X, Gu Y, Wang W, Guo W, Wang P, Du P (2024). Corynoline alleviates hepatic ischemia-reperfusion injury by inhibiting NLRP3 inflammasome activation through enhancing Nrf2/HO-1 signaling. *Inflamm Res*., **73**(12): 2069-2085.

Gong Z, Xue L, Li H, Fan S, van Hasselt C A, Li D, Zeng X, Tong MCF and Chen GG (2024). Targeting Nrf2 to treat thyroid cancer. *Biomed Pharmacother*., **173**: 116324.

Guan T, Li N, Xu X, Xiong D, Wang B, Xiao L, Yang W, Chu G, Yusuf A, Zhang J and Yue W (2024). Involvement of the Keap1-Nrf2-ARE pathway in the antioxidant activity of sinomenine. *Arch Biochem Biophys*., **753**: 109928.

Hayashi M, Kuga A, Suzuki M, Panda H, Kitamura H, Motohashi H and Yamamoto M (2020). Microenvironmental activation of Nrf2 restricts the progression of Nrf2-activated malignant tumors. *Cancer Res*., **80**(16): 3331–3344.

Hsu WL, Wang CM, Yao CL, Chen SC, Nien CY, Sun YH, Tseng TY and Luo YH (2022). Blockage of Nrf2 and autophagy by L-selenocystine induces selective death in Nrf2-addicted colorectal cancer cells through p62-Keap-1-Nrf2 axis. *Cell Death Dis*., **13**(12): 1060.

Huang J, Zhu Y, Li S, Jiang H, Chen N, Xiao H, Liu J, Liang D, Zheng Q, Tang J and Meng X (2023). Licochalcone B confers protective effects against LPS-Induced acute lung injury in cells and mice through the Keap1/Nrf2 pathway. *Redox Rep*., **28**(1): 2243423.

islam MA, Medha MM, Nahar AU, Al Fahad MA, Siraj MA and Seidel V (2023). Cancer protective role of selected dietary polyphenols via modulating Keap1/Nrf2/ARE and interconnected signaling pathways. *Nutr Cancer*., **75**(4): 1065–1102.

Jiang L, Guo P, Ju J, Zhu X, Wu S and Dai J (2023). Inhalation of L-arginine-modified liposomes targeting M1 macrophages to enhance curcumin therapeutic efficacy in ALI. *Eur J Pharm Biopharm.*, **182**: 21–31.

Jiang S, Han J, Li T, Xin Z, Ma Z, Di W, Hu W, Gong B, Di S, Wang D and Yang Y (2017). Curcumin as a potential protective compound against cardiac diseases. *Pharmacol Res*., **119**: 373–383.

Kunzmann S, Huetten M, Ottensmeier B, Kramer BW and Fehrholz M (2022). A20 is increased in fetal lung in a sheep LPS model of chorioamnionitis. *Oxid Med Cell Longev.*, **2022**: 6421419.

Lee S and Hu L (2020). Nrf2 activation through the inhibition of Keap1-Nrf2 protein-protein interaction. *Med Chem Res.*, **29**(5): 846–867.

Liao D, Shangguan D, Wu Y, Chen Y, Liu N, Tang J, Yao D and Shi Y (2023). Curcumin protects against doxorubicin induced oxidative stress by regulating the Keap1-Nrf2-ARE and autophagy signaling pathways. *Psychopharmacology*, **240**(5): 1179–1190.

Li B, Jiang T, Liu H, Miao Z, Fang D, Zheng L and Zhao J (2019). Andrographolide protects chondrocytes from oxidative stress injury by activation of the Keap1-Nrf2-Are signaling pathway. *J Cell Physiol*., **234**(1): 561–571.

Li J, Baker J, Higham A, Shah R, Montero-Fernandez A,

Murray C, Cooper N, Lucas C, Fox C, Singh D and Lea S (2022). COPD lung studies of Nrf2 expression and the effects of Nrf2 activators. *Inflammophramacology*, **30**(4): 1431–1443.

Liu M, Li Z, Cui Q, Yan B, Achi JG, Zhao Y, Rong L, Du R (2024). Integrated serum pharmacochemistry and investigation of the anti-influenza A virus pneumonia effect of Qingjin Huatan decoction. J *Ethnopharmacol.* **323**:117701.

Liu S, Pi J and Zhang Q (2021). Mathematical modeling reveals quantitative properties of KEAP1-NRF2 signaling. *Redox Biol*., **47**: 102139.

Liu Y, Zhang X, Cao Y, Chen X, Zhu J and Zou Y (2023). Ferrostatin-1 ameliorated oxidative lipid damage in LPS-induced acute lung injury. *J Surg Res*., **290**: 266–275.

Li W and Pauluhn J (2017). Phosgene-induced acute lung injury (ALI): Differences from chlorine-induced ALI and attempts to translate toxicology to clinical medicine. *Clin Transl Med.*, **6**: 19.

Li Z, Pan H, Yang J, Chen D, Wang Y, Zhang H and Cheng Y (2023). Xuanfei Baidu formula alleviates impaired mitochondrial dynamics and activated NLRP3 inflammasome by repressing NF-κB and MAPK pathways in LPS-induced ALI and inflammation models. *Phytomedicine*, **108**: 154545.

Meldrum K, Moura JA, Doak SH and Clift MJ (2022). Dynamic fluid flow exacerbates the (Pro-) inflammatory effects of aerosolised engineered nanomaterials *in-vitro*. *Nanomaterials*, **12**(19): 3431.

Murakami S, Kusano Y, Okazaki K, Akaike T and Motohashi H (2023). NRF2 signalling in cytoprotection and metabolism. *Br J Pharmacol*., **2023**: 1–14.

Shakya A, Liu P, Godek J, Mckee NW, Dodson M, Anandhan A, Ooi A, Garcia JGN, Costa M, Chapman E and Zhang DD (2023). The NRF2-p97-NRF2 negative feedback loop. *Redox Biol*., **65**: 102839.

Shi Q, Li Z, Dong Y, Yang G and Li M (2023). LncRNA THRIL, transcriptionally activated by AP-1 and stabilized by METTL14-mediated m6A modification, accelerates LPS-evoked acute injury in alveolar epithelial cells. *Int Immunopharmacol*., **123**: 110740.

Silwedel C, Fehrholz M, Speer CP, Ruf KC, Manig S and Glaser K (2019). Differential modulation of pulmonary caspases: Is this the key to ureaplasma-driven chronic inflammation? *PLoS One*, **14**(5): e0216569.

Traber KE, Mizgerd JP (2025). The integrated pulmonary immune response to pneumonia. *Annu Rev Immunol*.**43**(1): 545-569.

Tu W, Wang H, Li S, Liu Q and Sha H (2019). The anti-inflammatory and anti-oxidant mechanisms of the Keap1/Nrf2/ARE signaling pathway in chronic diseases. *Aging Dis*., **10**(3): 637–651.

Ulasov A, Rosenkranz AA, Georgiev GP and Sobolev AS (2022). Nrf2/Keap1/ARE signaling: Towards specific regulation. *Life Sci*., **291**: 120111.

Wang Q, Botchway BOA, Zhang Y and Liu X (2022). Ellagic acid activates the Keap1-Nrf2-ARE signaling pathway in improving Parkinson's disease: A review. *Biomed Pharmacother*., **156**: 113848.

Wang Y, Dong H, Qu H, Cheng W, Chen H, Gu Y, Jiang H, Xue X and Hu R (2024), Biomimetic lung-targeting nanoparticles with antioxidative and Nrf2 activating properties for treating ischemia/reperfusion-induced acute lung injury. *Nano Lett*., **24**(7): 2131–2141.

Willems CHMP, Zimmermann LJI, Sanders PJLT, Wagendorp M, Kloosterboer N, Tervaert JWC, Duimel HJQ, Verheyen FKCP and Van Iwaarden JF (2013). Alveolocapillary model system to study alveolar re-epithelialization. *Exp Cell Res*., **319**(1): 64–74.

Wu Y, Wang Y, Gong S, Tang J, Zhang J, Li F, Yu B, Zhang Y and Kou J (2020). Ruscogenin alleviates LPS-induced pulmonary endothelial cell apoptosis by suppressing TLR4 signaling. Biomed *Pharmacother*., **125**: 109868.

Wu Z, Luo Z, Sun, W, Shi Y and Ding Q (2023). Integrating network pharmacology and experimental validation to elucidate the mechanism of jiegeng decoction in improving allergic asthma. *Acs Omega*, **8**(50): 48081–48090.

Xuan Z, Wu H, Zhang S, Wang Y, Chen M, Gui S, Wang J and Yu Y (2024). *Platycodon grandiflorus* decoction attenuates lipopolysaccharide-induced acute lung injury via the PI3K/Akt/NF-κB pathway. *J Funct Foods*., **121**: 106448.

Xu F, Yuan J, Tian S, Chen Y and Zhou F (2020). MicroRNA-92a serves as a risk factor in sepsis-induced ARDS and regulates apoptosis and cell migration in lipopolysaccharide-induced HPMEC and A549 cell injury. *Life Sci*., **256**: 117957.

Xu Y, Wang X, Han D, Wang J, Luo Z, Jin T, Shi C, Zhou X, Lin L and Shan J (2022). Revealing the mechanism of Jiegeng decoction attenuates bleomycin-induced pulmonary fibrosis via PI3K/Akt signaling pathway based on lipidomics and transcriptomics. *Phytomedicine*, **102**: 154207.

Zhao Y, Zhou Y, Zhang W, Liu M, Duan J, Zhang X, Ma Q, Wang Y, Zhang Y, Guo Z, Zhang T, Zuo W (2025). Cloned airway basal progenitor cells to repair fibrotic lung through re-epithelialization. *Nat Commun*. **16**(1):1303